

RESEARCH

Open Access



# A CT-based radiomics model for predicting lymph node metastasis in hepatic alveolar echinococcosis patients to support lymph node dissection

Yinshu Zhou<sup>2†</sup>, Pengcai Feng<sup>1†</sup>, Fengyuan Tian<sup>1†</sup>, Hin Fong<sup>2</sup>, Haoran Yang<sup>3</sup> and Haihong Zhu<sup>1\*</sup>

## Abstract

**Background** Hepatic alveolar echinococcosis (AE) is a severe zoonotic parasitic disease, and accurate preoperative prediction of lymph node (LN) metastasis in AE patients is crucial for disease management, but it remains an unresolved challenge. The aim of this study was to establish a radiomics model for the preoperative prediction of LN metastasis in hepatic AE patients.

**Methods** A total of 100 hepatic AE patients who underwent hepatectomy and hepatoduodenal ligament LN dissection at Qinghai Provincial People's Hospital between January 2016 and August 2023 were included in the study. The patients were randomly divided into a training set and a validation set at an 8:2 ratio. Radiomic features were extracted from three-dimensional images of the hepatoduodenal ligament LNs delineated on arterial phase computed tomography (CT) scans of hepatic AE patients. Least absolute shrinkage and selection operator (LASSO) regression was applied for data dimensionality reduction and feature selection. Multivariate logistic regression analysis was performed to develop a prediction model, and the predictive performance of the model was evaluated using receiver operating characteristic (ROC) curves, calibration curves, and decision curve analysis (DCA).

**Results** A total of 7 radiomics features associated with LN status were selected using LASSO regression. The classification performances of the training set and validation set were consistent, with area under the operating characteristic curve (AUC) values of 0.928 and 0.890, respectively. The model also demonstrated good stability in subsequent validation.

**Conclusion** In this study, we established and evaluated a radiomics-based prediction model for LN metastasis in patients with hepatic AE using CT imaging. Our findings may provide a valuable reference for clinicians to determine the occurrence of LN metastasis in hepatic AE patients preoperatively, and help guide the implementation of individualized surgical plans to improve patient prognosis.

**Keywords** Hepatic alveolar echinococcosis, Lymph node metastasis, Radiomics, Machine learning

<sup>†</sup>Yinshu Zhou, Pengcai Feng, and Fengyuan Tian contributed equally to this work and share first co-authorship.

\*Correspondence:

Haihong Zhu  
zhuhaihong1214@126.com

Full list of author information is available at the end of the article



## Introduction

Alveolar echinococcosis (AE), a grave zoonotic parasitic disease, continues to pose a global health threat. Hepatic AE is particularly prevalent in regions with flourishing livestock industries and robust nomadic communities, with contributing factors including the local environment, hygiene practices, and socioeconomic conditions [1].

When an intermediate host, such as humans or sand rats, ingests food or water contaminated with *Echinococcus multilocularis* tapeworm eggs, these eggs will develop into oncospheres under the action of the host's digestive juices. Then, these oncospheres penetrate the intestinal wall, enter the portal vein, and ultimately settle in the liver to develop hepatic AE [2]. The growth characteristics of hepatic AE, akin to that of a neoplasm, have led to the development of the moniker "parasitic cancer", due to its proliferative and infiltrative nature, invasion of both adjacent tissues and organs, and metastasis to regional lymph nodes (LNs) through the deep and shallow drainage routes through the liver [3].

Current treatment protocols for hepatic AE primarily involve radical liver resection and drug therapy [4, 5]. In patients with hepatic AE with LN metastasis, regional LN dissection is also a requisite treatment measure [6]. Prior research has indicated that patients who undergo liver transplantation for end-stage hepatic AE without LN dissection often experience graft reinfection, underscoring the potential risk of persistent infection caused by LN metastasis [7].

Computed tomography (CT), a common preoperative examination technique, can be used to effectively visualize enlarged LNs [8]. However, its ability to discern the nature of the LN based on morphological attributes such as shape, size, and necrosis is limited, fails to meet the precision required for diagnosis and treatment. Therefore, it struggles to distinguish between reactive hyperplastic LNs resulting from chronic inflammation and infected LNs [9]. Current preoperative imaging techniques exhibit a low detection rate for LN metastasis, leading to a lack of study that can accurately predict LN metastasis in hepatic AE. While postoperative pathological assessment is the gold standard, it has limitations in clinical applications due to its delayed nature. Thus, the preoperative prediction of LN metastasis in hepatic AE patients is crucial for patient prognosis [10].

Radiomics, an emerging discipline within the medical field, utilizes high-throughput feature extraction to transform medical images into high-dimensional data for disease analysis and treatment decisions [11–13]. In this study, we employed CT radiomics to predict LN metastasis in hepatic AE patients, providing a rich source

of information for identifying the nature of LNs and enabling personalized treatment strategies [14].

## Methods

### Study design and patients

This retrospective study was approved by the Ethics Committee of Qinghai Provincial People's Hospital. Informed consent was waived due to the retrospective nature of the study. All methods were implemented in accordance with the Helsinki Declaration and relevant guidelines and regulations. The medical records of 162 hepatic AE patients who underwent hepatectomy and hepatoduodenal ligament LN dissection at Qinghai Provincial People's Hospital from June 2016 to August 2023 were retrieved from the hospital information system. Patient age, sex, PNM staging, and imaging data were collected. The inclusion criteria were as follows: (1) patients with a first diagnosis of hepatic AE confirmed by postoperative pathology. (2) Abnormal hepatic hilar LNs were found on preoperative CT. (3) Patients who have undergone hepatic hilar LNs dissection or removal of abnormal LNs. To maintain the rigor of our research methodology, the exclusion criteria were as follows: (1) comorbidities such as liver cirrhosis and chronic hepatitis may affect the results of the analysis. (2) Low-quality CT images were excluded to ensure that the data used for developing the models were reliable. (3) Patients whose clinical information was incomplete or who were lost to follow-up. Ultimately, 100 patients were included in the study. Postoperative pathological results served as the gold standard; 36 patients were diagnosed with LN metastasis, and 64 patients were diagnosed with reactive LN hyperplasia. The patients were randomly assigned to the training or validation set at a ratio of 8:2, which resulted in 80 patients being allocated to the training set and 20 patients being allocated to the validation set. The flowchart shows the details of patient selection and process (Fig. 1).

### CT image acquisition

The scanning range extended from the diaphragm to the pubic symphysis. The parameters for abdominal enhanced scanning were set according to the "CT Examination Technology Expert Consensus" of 2016: 120 kV, automatic milliampere technology for effective tube current, helical scanning with a pitch of 0.98–1.37, tube rotation speed of 0.6–0.8 s/rotation, detector width of 64×0.625 mm, and field of view of 300 mm×350 mm. The contrast agent used was iodixanol 300 (iodine concentration 300 mg/mL), which was injected through a high-pressure injector via the intravenous route at a flow rate of 3.0 mL/s. The dose administered was 1.5 mL/kg body weight, followed by a 30 mL saline flush. Arterial

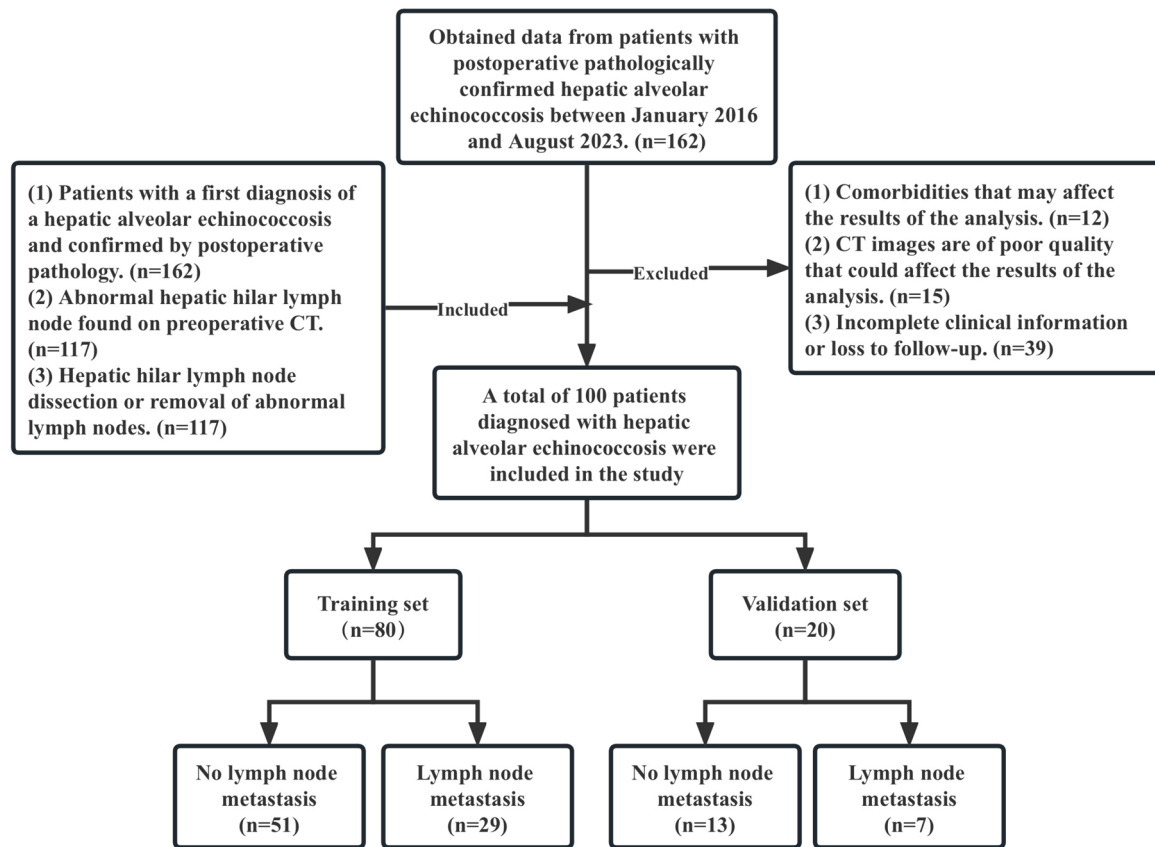


**Fig. 1** Flowchart illustrating the selection criteria

and venous phase scans were performed at 30 and 55 s, respectively, after the injection of the contrast agent.

#### Image segmentation and radiomics feature extraction

All the data were imported into 3D Slicer 5.2.2 software, and two radiologists independently measured and delineated the CT images using a double-blind method. 3D Slicer software was used to generate a 1.25-mm-thick image of the preoperative enhanced CT arterial phase. The LNs along the hepatoduodenal ligament, as indicated in the pathological report of patients with liver hepatic AE, are delineated in three-dimensional. The built-in “PyRadiomics” package of 3D Slicer was utilized to extract features from the delineated images. The extracted features are categorized into four groups: (1) first-order features based on the voxel intensity distribution within the region of interest, including the maximum, median, minimum, and mean voxel intensities; (2) shape features based on the delineated region of interest, such as the maximum surface area of the lesion; (3) texture features, including the gray-level co-occurrence matrix and gray-level size zone matrix;

and (4) high-order statistical features, such as wavelet decomposition features based on texture features. In this study, the intraclass correlation coefficient (ICC) was used to assess the interobserver reliability of the radiomic feature extraction method, with an ICC > 0.75 indicating good consistency.

#### Selection of radiomics features

To identify significant features among a large number of radiomic features, the radiomic features with an ICC > 0.75 in the training set were initially screened using one-way analysis of variance (ANOVA). The features exhibiting significant statistical significance were then included in the least absolute shrinkage and selection operator (LASSO) regression model to eliminate collinearity and select the most valuable features[15]. The model selected the  $\lambda$  value with the minimum mean squared error (MSE) plus one standard error (SE) in tenfold cross-validation, aiming to shrink as many feature coefficients to zero as possible and obtain a model with the fewest parameters.

### Development and evaluation of radiomics model

A radiomics model was established using logistic regression, incorporating the final features obtained after the second screening [16]. The variance inflation factor (VIF) was calculated to determine if there was significant multicollinearity among the variables in the radiomics model. Variables with a VIF greater than 10 indicated significant multicollinearity. Nomogram was used to visualize radiomics model [17]. The area under the curve (AUC) for the receiver operating characteristic (ROC) curve of the training set and validation set was used to evaluate the predictive performance of the radiomics model. Additionally, calibration curve and decision curve analysis (DCA) were employed to further assess the predictive accuracy and application value of the model [18, 19].

### Statistical analysis

Statistical analysis was conducted using R software (version 4.3.2). The "stats" package was utilized to construct the logistic regression model, the "glmnet" package was used to construct the LASSO model, the "rms" package was utilized to plot the nomogram and calibration curve, the "pROC" package was utilized to generate the ROC curve, and the "rmda" package was employed to plot the DCA. The normality test was performed for each of the measured data, utilizing the independent samples t test if the data followed a normal distribution and vice versa, utilizing the Mann–Whitney U test. The Chi-square test was used for comparing categorical data. All tests were two-sided, and a p value less than 0.05 was considered to indicate statistical significance.

## Results

### Patient characteristics

All suspicious LNs were confirmed by postoperative pathological results, with 36 cases of hepatic AE LN metastasis and 64 cases of reactive LN hyperplasia. There were no statistically significant differences in sex, age, PNM staging, lesion location, or lesion size between the two groups of patients ( $P > 0.05$ ) (Table 1).

### Establishment of the radiomics model

A total of 874 radiomic features were extracted from each lesion in the training set, all with an ICC greater than 0.75 (range: 0.861–1). A total of 112 of these genes passed the ANOVA test and were included in the LASSO regression model (Fig. 2A). We introduced a regularization parameter  $\lambda$  and used tenfold cross-validation to select the optimal  $\lambda$  value for the LASSO model based on the 1-SE criteria, with the selected  $\lambda = 0.105$  (Fig. 2B). Coefficient path plots were generated based on  $\log(\lambda)$ , and ultimately, seven radiomic features with non-zero coefficients were identified, namely, LeastAxisLength, MajorAxisLength, SurfaceVolumeRatio, Median, Skewness, DependenceEntropy, and ZoneEntropy (Fig. 2C). The radiomics score was calculated by using the following formula: Radiomics score =  $-8.375596 + 0.028959 * \text{LeastAxisLength} + 0.003892 * \text{MajorAxisLength} - 4.610770 * \text{SurfaceVolumeRatio} - 0.038589 * \text{Median} + 0.996096 * \text{Skewness} + 2.018510 * \text{DependenceEntropy} + 0.303349 * \text{ZoneEntropy}$  (Fig. 2D). The scatter plots of the radiomics score for each patient in the training and validation sets are shown in Additional file 1: Fig. S1. The detailed radiomic features of all patients can be found in Additional file 2: Table S1.

**Table 1** Demographic data of the patients

Parameter	No lymph node metastasis N = 64	Lymph node metastasis N = 36	T value/ $\chi^2$	p-value
Gender				
Female	38 (59.4%)	21 (58.3%)	0.010	0.919
Male	26 (40.6%)	15 (41.7%)		
Age (mean $\pm$ SD, yr)	31.7 $\pm$ 13.1	34.7 $\pm$ 15.0	-0.999	0.321
PNM staging				
Stage 2 (P2N0M0)	1 (1.56%)	0 (0.00%)		0.390
Stage 3a (P3N0M0)	3 (4.69%)	2 (5.56%)		
Stage 3b (P1–3N1M0) (P4N0M0)	38 (59.4%)	16 (44.4%)		
Stage 4 (P4N1M0) (P1–4N0–1M1)	22 (34.4%)	18 (50.0%)		
Location of lesions				
Left	17 (26.6%)	4 (11.1%)	3.316	0.069
Right	47 (73.4%)	32 (88.9%)		
Lesion size (mean $\pm$ SD, m <sup>2</sup> )	111 $\pm$ 68.1	96.0 $\pm$ 68.5	1.063	0.291

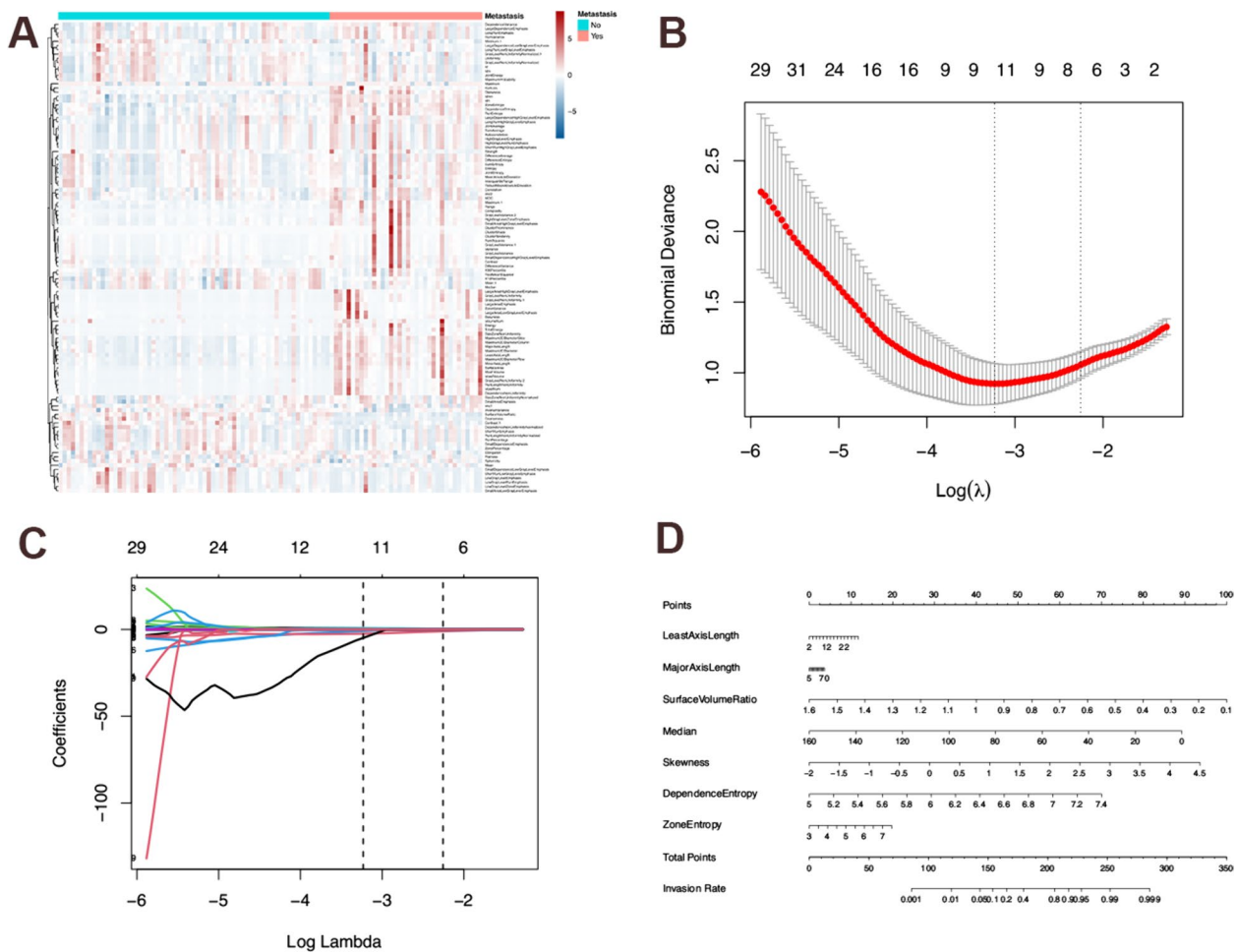


**Fig. 2** Signature selection using LASSO regression and logistic regression models in the training set. **A** Heatmap of correlation between radiomics signatures and LN status. **B**  $\lambda$  selection was used in the LASSO model with tenfold cross-validation by the one standard error of the minimum criteria, the value of  $\lambda$  is 0.105. The left and right dotted lines correspond to the minimum criterion and one standard error of the minimum criteria. **C** The path plots of coefficient contraction for the radiomics signatures with  $\text{log}(\lambda)$  as the horizontal coordinate shows that 7 signatures will be left to have non-zero coefficients when the value of  $\lambda$  is 0.105. The left and right dotted lines correspond to the minimum criterion and one standard error of the minimum criteria. **D** The radiomics nomogram was developed with the training set

### Evaluation of the predictive performance of the radiomics model

The VIFs of the seven variables in the radiomics model ranged from 1.276 to 6.422 (Additional file 3: Table S2), indicating that there was no severe collinearity among them. Radiomics image data were collected for two patients, and the status of suspicious LNs was determined, as shown in Fig. 3. The predictive efficacy of the radiomics model is shown in Table 2, with a sensitivity of 0.897 and a specificity of 0.843 in the training set and a sensitivity of 0.857 and a specificity of 0.923 in the validation set. The predictive results of the two sets are consistent. The ROC analysis results

showed good classification performance in the training set ( $\text{AUC} = 0.928$ ) and validation set ( $\text{AUC} = 0.890$ ). In both sets, the calibration curves showed a close match between the predicted probabilities and actual probabilities, demonstrating good discrimination and calibration capabilities. The DCA showed that the model's performance was consistently greater than the extreme curve throughout the entire range, further indicating its good clinical applicability (Fig. 4). Overall, our radiomics model may have good predictive performance and can accurately differentiate whether suspicious LNs have hepatic AE metastasis preoperatively.

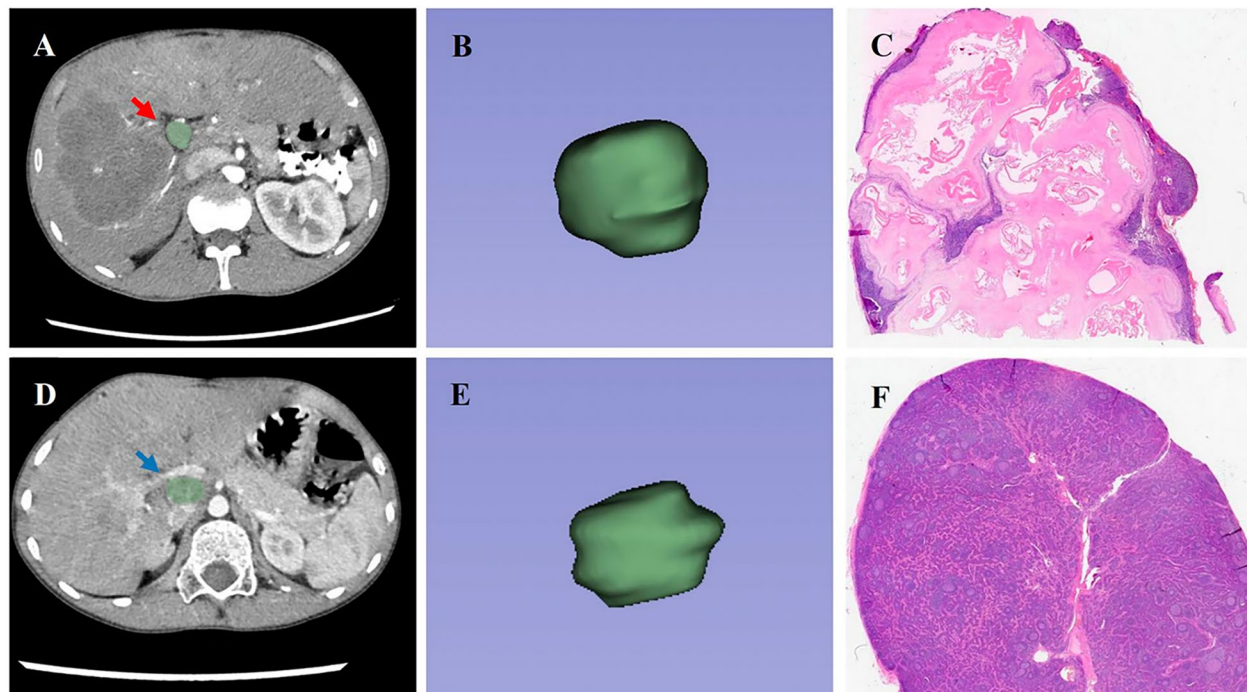


**Fig. 3** **A, B,** and **C** are a 37-year-old female patient with AE metastatic LN confirmed on postoperative pathology; **D, E,** and **F** are a 23-year-old male patient with reactive hyperplastic LN confirmed on postoperative pathology. **A** The arterial phase CT scan shows the suspicious LN and an ROI (red arrow) is outlined along the edge of the LN. **B** The figure shows a three-dimensional ROI along the layer-by-layer outlining of the entire LN. **C** Hematoxylin–eosin staining with 1× magnification, and observation showing the suspicious LN has AE metastasis. **D** CT scan in the arterial phase showing the suspicious LN and outlining the ROI along the edge (blue arrow). **E** The figure shows a three-dimensional ROI along the layer-by-layer outlining of the entire LN. **F** Hematoxylin–eosin staining with 1× magnification, and the observation shows that the suspicious LN is a reactive hyperplastic LN

**Table 2** Prediction performance of the LR model

Parameter	Training set	Validation set
Cutoff	0.318	0.318
Recall	0.897	0.857
Precision	0.765	0.857
Sensitivity	0.897	0.857
Specificity	0.843	0.923
Accuracy	0.863	0.900
F1	0.825	0.857
Brier	0.105	0.077
AUC (95% CI)	0.928 (0.874–0.983)	0.890 (0.731–1.000)

## Discussion

According to the consensus of international experts, hepatectomy is the preferred curative treatment for hepatic AE patients, but it does not explicitly specify how to handle potentially infected LNs [6]. Unfortunately, in advanced or extensively lesioned hepatic AE, lymphatic drainage pathways from the liver, both deep and superficial, often lead to regional LN metastasis [20]. A

meta-analysis of 417 studies was mentioned, followed up after categorizing them into two groups based on whether LN dissection was performed. The comparison revealed a significantly better prognosis for patients who had undergone LN dissection [21]. In patients with advanced AE who underwent liver transplantation without LN dissection, recurrence of infection in the transplant occurred several years later, suggesting that LN metastasis might pose a potential risk for persistent infection [22]; this indicates that neglecting the treatment of patients' LNs may have a serious impact on their prognosis, but there are limitations in distinguishing patients who require LN dissection at present [23].

Currently, the identification of preoperative LNs is usually achieved by conventional imaging methods, which are subject to observer bias and characterized by low sensitivity and specificity [24]. Nonenhanced LN enhancement, nodules within the LN, and "sand-like" calcification are important CT signs of AE LN metastasis. However, in our daily clinical work, we observed that some patients with pathological findings suggestive of AE LN metastasis may not present these CT markers [25]. For LNs suspected of having metastasis, biopsy

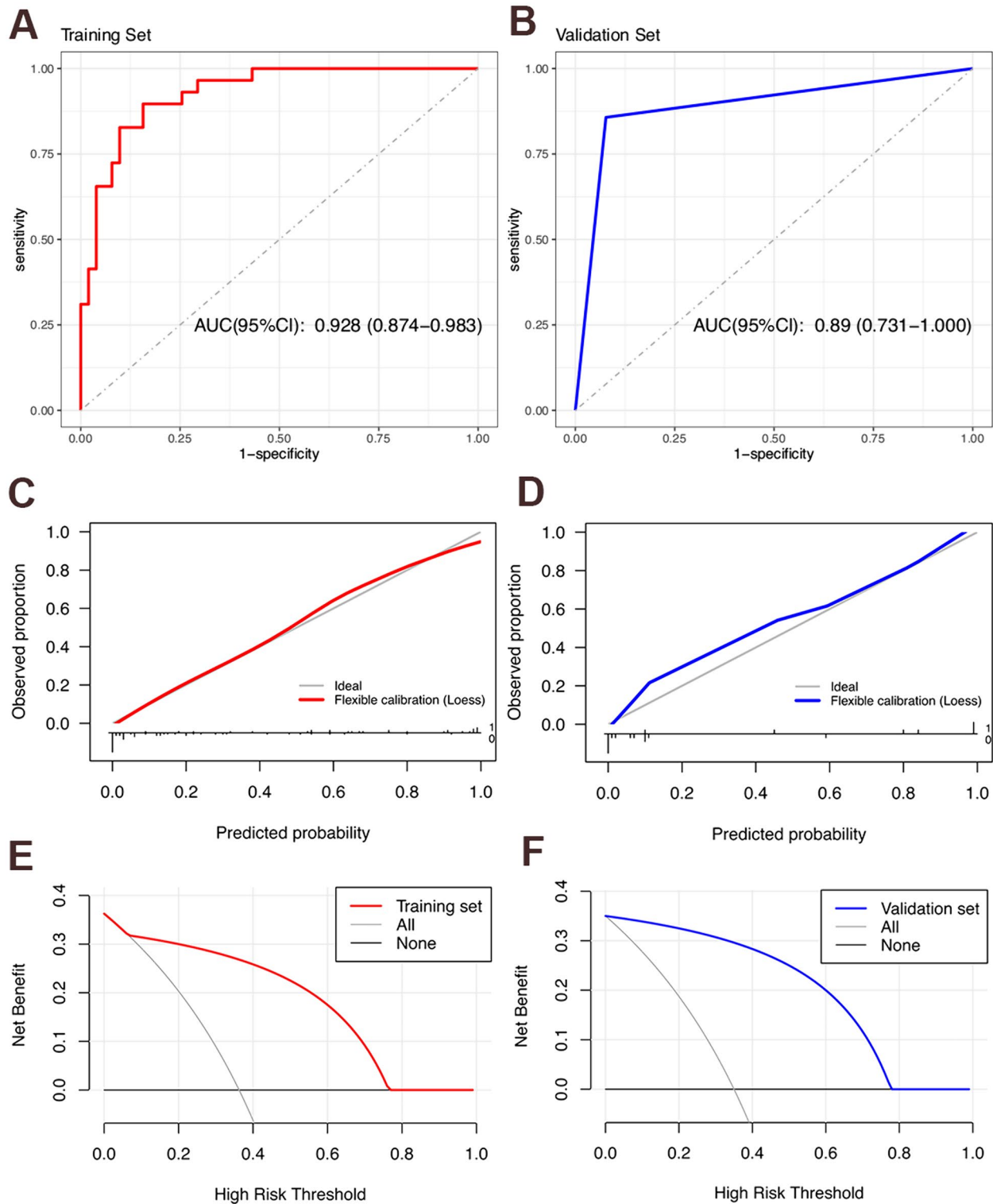


**Fig. 4** The predictive efficacy of the radiomics model is validated in the training set and validation set. The prediction effectiveness of the training set (A) and validation set (B) is shown in the ROC curves. Radiomics model calibration curves for training set (C) and validation set (D) showing the consistency of actual and predicted probabilities. DCA of training set (E) and test set (F) shows the relationship between net gain and threshold probability

is the gold standard for diagnosis, but it is an invasive procedure with certain risks. The perihepatic LNs are quite deep and numerous, which makes it impossible to obtain samples from the suspected LNs one by one. Therefore, there is an urgent need for a new and effective method to distinguish whether LN metastases have occurred, facilitating the development of a more personalized treatment plan for patients.

Radiomics is a method of image analysis that quantitatively assesses features such as shape, texture, and intensity to yield insights into diseases or tissues [26]. Radiomics research has advanced significantly, integrating diverse medical imaging data, supplying large datasets for machine learning, and enhancing the accuracy and efficiency of automated analyses [11]. The application of radiomics in predicting tumor LN metastasis preoperatively has gained recognition and demonstrated superior predictive power compared to traditional models [27]. To reduce bias, our study focused on the hepatoduodenal ligament LN, the most common site of metastasis. Using radiomics, we analyzed CT-enhanced arterial phase images of suspicious LNs for which the status could not be confirmed. AE proliferates continuously, causing complete destruction of the LN to form a necrotic granulomatous mass, with no enhancement being an important signature CT image feature [28]. Moreover, the LNs in the arterial phase were clearly delineated from the surrounding tissues and easily outlined. LASSO regression was utilized to reduce the number of dimensions in the images and select seven optimal features. LeastAxisLength and MajorAxisLength are classified as shape features, which in this study represent the size of the LNs. Larger values suggest a greater likelihood of metastatic LNs. The SurfaceVolumeRatio also falls under the shape feature, reflecting the irregularity of the LN surface. Its value is inversely proportional to the possibility of AE metastasis, indicating that the surfaces of metastatic LNs are relatively smooth. First-order statistics include Median and Skewness, which reflect the intensity and asymmetrical distribution of the lesion image pixels, providing insights into the tissue density or nature within the lesion. In this study, the pixel intensity of metastatic LNs was lower, indicating that the density inside the affected lymph nodes was lower and that the distribution was asymmetrical. DependenceEntropy and ZoneEntropy, which extract entropy values from the image texture, are texture features. In this study, higher DependenceEntropy and ZoneEntropy were associated with an increased risk of AE LN metastasis, indicating significant complexity and randomness in the relationships among pixels within the lesion image [29, 30]. The incorporation of these signatures into logistic

regression to construct a nomogram revealed that radiomics score is significantly correlated with the risk of hepatic AE LNs metastasis. ROC curves, calibration curves, and DCA further confirmed the predicted stability of radiomics model. Based on these findings, our radiomics model may assist in identifying AE metastatic LNs. In addition, previous studies have shown that clinical features are not associated with LN metastasis in patients with hepatic AE [31], consistent with the data in this study (Table 1). Therefore, we did not include clinical features in the final model. In the future, we will consider enhancing the predictive performance of the model by combining additional parameters, such as laboratory indices [32].

Through the analysis of a large number of specimens obtained after LN dissection, we discovered that some LNs with reactive hyperplasia due to long-term chronic inflammation are often identified as suspicious LNs before surgery [33]. This peculiar situation may arise because a large amount of inflammatory substances generated by hepatic AE spread to regional LNs through the lymphatic system, thereby triggering varying degrees of immune response. Consequently, local fibrosis, chronic inflammation, LN edema, and hyperplasia occur, ultimately leading to the formation of characteristic granulomatous changes [34]. Reactive LN hyperplasia resulting from chronic inflammation can be actively monitored and observed. Engaging in the blind dissection of all suspicious LNs may have several detrimental consequences for the patient, including surgical risks, prolonged postoperative recovery, complications, and additional medical expenses. Furthermore, previous studies have demonstrated that AEs can metastasize via lymphatic drainage, and if only hepatectomy is performed without considering that removal of regional LNs may leave parasitic tissue behind, even if it is not apparent, we believe that LN dissection is essential for patients with AE metastasis. The long-term prognosis of patients with reactive hyperplastic lymph nodes and metastatic lymph nodes after lymph node dissection was compared in another follow-up study of up to 10 years, and the results demonstrated no significant difference [31]; this indicates that, as long as LN dissection is performed on patients with metastatic LNs, their prognosis can be at least as good as that of non-metastatic patients. Additionally, although LN dissection does prolong the duration of the operation, it is not directly associated with postoperative complications. In summary, radical liver resection combined with regional LN dissection is a safe, feasible, and effective approach for treating hepatic AE.

Nevertheless, our study has several limitations. Firstly, the possible sites of LN metastasis in hepatic AE are the areas near the hepatoduodenal ligament,



common hepatic artery, gastric lesser curvature, and celiac trunk [35]. This study focused only on the most common hepatoduodenal ligament LN without including other sites; although the probability of metastasis to other LNs being very small, this limitation might underestimate the true incidence of LN metastasis. Future research that extends to these additional sites could improve the predictive accuracy and clinical relevance of radiomics model. Secondly, this was a single-center, retrospective study. Despite processing the data robustly and conducting verification, the insufficient sample size may have led to bias in the results from the actual circumstances. Our subsequent step will involve conducting multicenter, prospective studies while continuing to follow up with previous patients to further validate our findings. Finally, we exclusively selected CT-enhanced phase images for the extraction of radiomic features and did not incorporate magnetic resonance, ultrasound, or other images. The inability to extract complementary information from different imaging technologies might limit the application of the model in complex cases, especially where CT alone cannot fully reveal the details of the lesion [36]. Future research should consider a variety of imaging data to provide a more robust foundation for radiomic analysis.

## Conclusion

In this study, we successfully established the first model for predicting LN metastasis in patients with hepatic AE and confirmed its favorable predictive efficacy, which not only helps physicians determine the presence of LN metastasis, but also provides innovative insight for treatment decisions. This result is complementary to the personalized treatment of hepatic AE, and we look forward to the future application of this model in clinical practice to improve the long-term prognosis of patients.

## Abbreviations

AE	Alveolar echinococcosis
LN	Lymph node
CT	Computed tomography
ICC	Intraclass correlation coefficient
ANOVA	Analysis of variance
LASSO	The least absolute shrinkage and selection operator
MSE	Mean squared error
SE	Standard error
VIF	The variance inflation factor
AUC	The area under the curve
ROC	The receiver operating characteristic
DCA	Decision curve analysis

## Supplementary Information

The online version contains supplementary material available at <https://doi.org/10.1186/s40001-024-01999-x>.

Additional file 1: **Fig. S1** The scatter plot of the radiomics score for each patient in training set (A) and validation set (B). The red markers indicate

patients without AE LN metastasis; the blue markers indicate patients with LN metastasis.

Additional file 2: **Table S1** The detailed radiomic features of all patients.

Additional file 3: **Table S2** The VIFs of the seven variables in the radiomics model.

## Acknowledgements

We thank all the researchers who contributed to this study.

## Author contributions

FT and YZ designed the study and performed the data analysis; HF and HY conducted the experiments and collected the data; HZ and PF provided critical resources and supervised the study; FT and YZ wrote the manuscript, with HF, HY, and PF providing substantial revisions. All authors have read and agreed to the published version of the manuscript.

## Funding

This research was funded by "KunLun talents High-end Innovation and Entrepreneurship Talent Program" of Qinghai Province (Youth Talent character [2021] No. 13) and Qinghai University Medical Department 2023 young and middle-aged teacher Research Fund Project (2023-ky-10).

## Availability of data and materials

Data is provided within the manuscript or supplementary information files.

## Declarations

### Ethics approval and consent to participate

This retrospective study was approved by the Ethics Committee of Qinghai Provincial People's Hospital (code: (2023)-277). Informed consent was waived due to the retrospective nature of the study.

### Consent for publication

Not applicable.

### Competing interests

The authors declare no competing interests.

### Author details

<sup>1</sup>General Surgery Department, Qinghai Provincial People's Hospital, Xining 810000, Qinghai, China. <sup>2</sup>First School of Clinical Medicine, Jinan University, No.601 Huangpu Avenue West, Guangzhou 510632, China. <sup>3</sup>School of Medicine, Jinan University, No.601 Huangpu Avenue West, Guangzhou 510632, China.

Received: 25 January 2024 Accepted: 27 July 2024

Published online: 07 August 2024

## References

1. Brunetti E, Kern P, Vuitton DA. Expert consensus for the diagnosis and treatment of cystic and alveolar echinococcosis in humans. *Acta Trop*. 2010;114(1):1–16.
2. Torgerson PR, Keller K, Magnotta M, Ragland N. The global burden of alveolar echinococcosis. *PLoS Negl Trop Dis*. 2010;4(6): e722.
3. Ohtani O, Ohtani Y. Lymph circulation in the liver. *Anat Rec (Hoboken)*. 2008;291(6):643–52.
4. Wen H, Vuitton L, Tuxun T, Li J, Vuitton DA, Zhang W, et al. Echinococcosis: advances in the 21st Century. *Clin Microbiol Rev*. 2019. <https://doi.org/10.1128/CMR.00075-18>.
5. Li C, Zhang Y, Pang M, Zhang Y, Hu C, Fan H. Metabolic mechanism and pharmacological study of albendazole in secondary hepatic alveolar echinococcosis (HAE) model rats. *Antimicrob Agents Chemother*. 2024;68(5): e0144923.

6. Buttenschoen K, Kern P, Reuter S, Barth TF. Hepatic infestation of *Echinococcus multilocularis* with extension to regional lymph nodes. *Langenbecks Arch Surg*. 2009;394(4):699–704.
7. Shen S, Kong J, Zhao J, Wang W. Outcomes of different surgical resection techniques for end-stage hepatic alveolar echinococcosis with inferior vena cava invasion. *HPB*. 2019;21(9):1219–29.
8. Wang J, Xing Y, Ren B, Xie WD, Wen H, Liu WY. Alveolar echinococcosis: correlation of imaging type with PNM stage and diameter of lesions. *Chin Med J (Engl)*. 2011;124(18):2824–8.
9. Jiang Y, Li J, Wang J, Xiao H, Li T, Liu H, et al. Assessment of vascularity in hepatic alveolar echinococcosis: comparison of quantified dual-energy CT with histopathologic parameters. *PLoS ONE*. 2016;11(2): e0149440.
10. Graeter T, Kratzer W, Oetzuerk S, Haenle MM, Mason RA, Hillenbrand A, et al. Proposal of a computed tomography classification for hepatic alveolar echinococcosis. *World J Gastroenterol*. 2016;22(13):3621–31.
11. Bian Y, Zheng Z, Fang X, Jiang H, Zhu M, Yu J, et al. Artificial intelligence to predict lymph node metastasis at CT in pancreatic ductal adenocarcinoma. *Radiology*. 2023;306(1):160–9.
12. Crombé A, Lucchesi C, Bertolo F, Kind M, Spalato-Ceruso M, Toulmonde M, et al. Integration of pre-treatment computational radiomics, deep radiomics, and transcriptomics enhances soft-tissue sarcoma patient prognosis. *NPJ Precis Oncol*. 2024;8(1):129.
13. Meng X, Xu H, Liang Y, Liang M, Song W, Zhou B, et al. Enhanced CT-based radiomics model to predict natural killer cell infiltration and clinical prognosis in non-small cell lung cancer. *Front Immunol*. 2023;14:1334886.
14. Gillies RJ, Kinahan PE, Hricak H. Radiomics: images are more than pictures. *They Data Radiology*. 2016;278(2):563–77.
15. Alhamzawi R, Ali HTM. The Bayesian adaptive lasso regression. *Math Biosci*. 2018;303:75–82.
16. Huang YQ, Liang CH, He L, Tian J, Liang CS, Chen X, et al. Development and validation of a radiomics nomogram for preoperative prediction of lymph node metastasis in colorectal cancer. *J Clin Oncol*. 2016;34(18):2157–64.
17. O'Brien RM. A caution regarding rules of thumb for variance inflation factors. *Qual Quant*. 2007;41(5):673–90.
18. Vickers AJ, Cronin AM, Elkin EB, Gonen M. Extensions to decision curve analysis, a novel method for evaluating diagnostic tests, prediction models and molecular markers. *BMC Med Inform Decis Mak*. 2008;8:53.
19. Kramer AA, Zimmerman JE. Assessing the calibration of mortality benchmarks in critical care: the Hosmer-Lemeshow test revisited. *Crit Care Med*. 2007;35(9):2052–6.
20. Eckert J, Thompson RC, Mehlhorn H. Proliferation and metastases formation of larval *Echinococcus multilocularis*. I. Animal model, macroscopical and histological findings. *Z Parasitenkd*. 1983;69(6):737–48.
21. Buttenschoen K, Gruener B, Carli Buttenschoen D, Reuter S, Henne-Bruns D, Kern P. Palliative operation for the treatment of alveolar echinococcosis. *Langenbecks Arch Surg*. 2009;394(1):199–204.
22. Bresson-Hadni S, Blagosklonov O, Knapp J, Grenouillet F, Sako Y, Delabrousse E, et al. Should possible recurrence of disease contraindicate liver transplantation in patients with end-stage alveolar echinococcosis? a 20-year follow-up study. *Liver Transpl*. 2011;17(7):855–65.
23. Hillenbrand A, Beck A, Kratzer W, Graeter T, Barth TFE, Schmidberger J, et al. Impact of affected lymph nodes on long-term outcome after surgical therapy of alveolar echinococcosis. *Langenbecks Arch Surg*. 2018;403(5):655–62.
24. Wang F, Zhang B, Wu X, Liu L, Fang J, Chen Q, et al. Radiomic nomogram improves preoperative T category accuracy in locally advanced laryngeal carcinoma. *Front Oncol*. 2019;9:1064.
25. Liu W, Delabrousse E, Blagosklonov O, Wang J, Zeng H, Jiang Y, et al. Innovation in hepatic alveolar echinococcosis imaging: best use of old tools, and necessary evaluation of new ones. *Parasite*. 2014;21:74.
26. Mayerhoefer ME, Materka A, Langs G, Häggström I, Szczypiński P, Gibbs P, et al. Introduction to radiomics. *J Nucl Med*. 2020;61(4):488–95.
27. Liu C, Ding J, Spuhler K, Gao Y, Serrano Sosa M, Moriarty M, et al. Preoperative prediction of sentinel lymph node metastasis in breast cancer by radiomic signatures from dynamic contrast-enhanced MRI. *J Magn Reson Imaging*. 2019;49(1):131–40.
28. Wang Q, Cui Y, Ren L, Wang H, Wang Z, Wang H, et al. Suspected regional lymph node metastasis in hepatic alveolar echinococcosis: a case report. *Iran J Parasitol*. 2020;15(1):138–41.
29. Lambin P, Rios-Velazquez E, Leijenaar R, Carvalho S, van Stiphout RG, Granton P, et al. Radiomics: extracting more information from medical images using advanced feature analysis. *Eur J Cancer*. 2012;48(4):441–6.
30. Abbasian Ardakani A, Bureau NJ, Ciaccio EJ, Acharya UR. Interpretation of radiomics features—a pictorial review. *Comput Methods Programs Biomed*. 2022;215: 106609.
31. Qiu H, Yang X, Shen S, Wang W. Relevance of regional lymph node invasion in radical hepatectomy and lymphadenectomy for alveolar echinococcosis. *Asian J Surg*. 2022;45(1):490–2.
32. Li T, Ito A, Nakaya K, Qiu J, Nakao M, Zhen R, et al. Species identification of human echinococcosis using histopathology and genotyping in north-western China. *Trans R Soc Trop Med Hyg*. 2008;102(6):585–90.
33. Reinehr M, Micheloud C, Grimm F, Kronenberg PA, Grimm J, Beck A, et al. Pathology of echinococcosis: a morphologic and immunohistochemical study on 138 specimens with focus on the differential diagnosis between cystic and alveolar echinococcosis. *Am J Surg Pathol*. 2020;44(1):43–54.
34. Ali-Khan Z, Siboo R, Gomersall M, Faucher M. Cystolytic events and the possible role of germinal cells in metastasis in chronic alveolar hydatidosis. *Ann Trop Med Parasitol*. 1983;77(5):497–512.
35. Feng X, Qi X, Yang L, Duan X, Fang B, Gongsang Q, et al. Human cystic and alveolar echinococcosis in the Tibet autonomous region (TAR) China. *J Helminthol*. 2015;89(6):671–9.
36. Yip SS, Aerts HJ. Applications and limitations of radiomics. *Phys Med Biol*. 2016;61(13):R150–166.

## Publisher's Note

Springer Nature remains neutral with regard to jurisdictional claims in published maps and institutional affiliations.